

## 1

## Basic HPLC Theory and Definitions: Retention, Thermodynamics, Selectivity, Zone Spreading, Kinetics, and Resolution

*Torgny Fornstedt, Patrik Forssén, and Douglas Westerlund*

Liquid chromatography is a very important separation method used in practically all chemistry fields. For many decades, it has played a key role in academic and industrial laboratories where it is used to analyze or purify components from complex mixtures. For example, it is used to separate proteins/drugs from impurities and to analyze drugs and endogenous components in biological materials. Most breakthroughs in biochemical and pharmaceutical sciences would probably not have been possible without chromatography.

Chromatography is generally considered to have been developed in the early twentieth century by the Russian botanist Tswett. He found that he could separate components from plant extracts by flushing a sample with organic solvents through a glass tube packed with an inorganic adsorbent. Distinct bands of various colors evolved and migrated at different rates down the column. The bands corresponding to the different plant pigments could be collected at the outlet at the bottom of the tube. Tswett chose to call his technique “chromatography,” which means “color writing” in Greek. The name has been kept for historical reasons, although it is not very descriptive of the method in general. His publications had, however, little impact, and the technique fell into oblivion for several decades.

Chromatography is based on the partitioning of solutes between two phases and is, therefore, related to simple liquid–liquid extraction. In chromatography, however, one phase (the mobile phase) is in constant movement relative to the other one (the stationary phase). The sample molecules are partitioned between the phases; those in the stationary phase are retained, whereas those in the mobile phase move. The interaction between the solutes and the stationary phase is most often based on adsorption. During a chromatographic separation, a solute normally partitions between the phases many thousand times. The basis of separation is that different kinds of molecules on average spend different amount of time in the stationary phase. Due to the large number of partitioning steps, chromatography has enormous resolving power and can separate mixtures of components with very similar physical properties. In the most common format, called column chromatography, the stationary phase is a highly porous solid material packed inside a cylindrical column (steel or glass), whereas the mobile phase is a liquid, a gas, or a supercritical fluid. If a successful separation has been

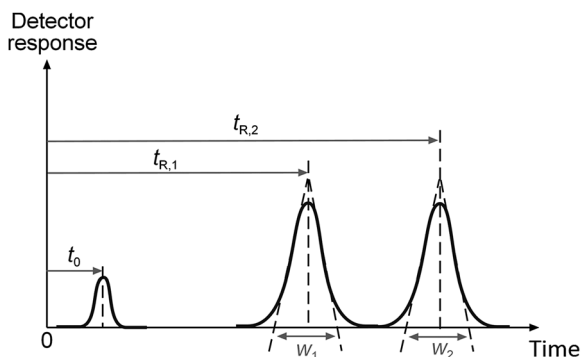


**Figure 1.1** Schematic representation of an ideal analytical chromatogram for a binary sample mixture with an unretained component ( $t_0$ ). The retention times of the peaks  $t_R$  are determined at the peak maxima and the peak widths  $W$  at the baseline.

made of a binary sample, this will in the ideal case result in the elution of two Gaussian-shaped concentration peaks (see Figure 1.1).

Mathematical models for chromatography were formulated in the 1940s [1] and in 1952 Martin and Synge were awarded the Nobel Prize in chemistry for their work on partition chromatography [2]. The work by Giddings [3] in the 1960s is also considered a milestone in the history of chromatography, for its stringent description of the causes of zone spreading (also called band broadening). The theory describes how the column should be designed and treated to result in efficient separations. The stationary-phase particles should have a small particle diameter, uniform geometry and small-size distribution, and should be homogeneously packed, and any extra column volume should be minimized. Academic scientists, and later manufacturers, followed these directions that resulted in improved liquid chromatography; for example, high-performance liquid chromatography (HPLC) in the 1970s illustrates the dramatic improvements achieved.

Chromatography is categorized after the type of mobile phase used, liquid, gas, or supercritical chromatography, which will be described in more detail in later chapters. In this chapter, we will focus on the basic theory necessary for a deeper understanding of the separation process but will also cover new trends in liquid chromatography today.

## 1.1

### Basic Definitions

In analytical chromatography, we want to obtain quantitative and/or qualitative information about one or several components in a sample mixture, whereas in preparative chromatography, the aim is to purify the individual components. The qualitative information is obtained from the retention times in an analytical

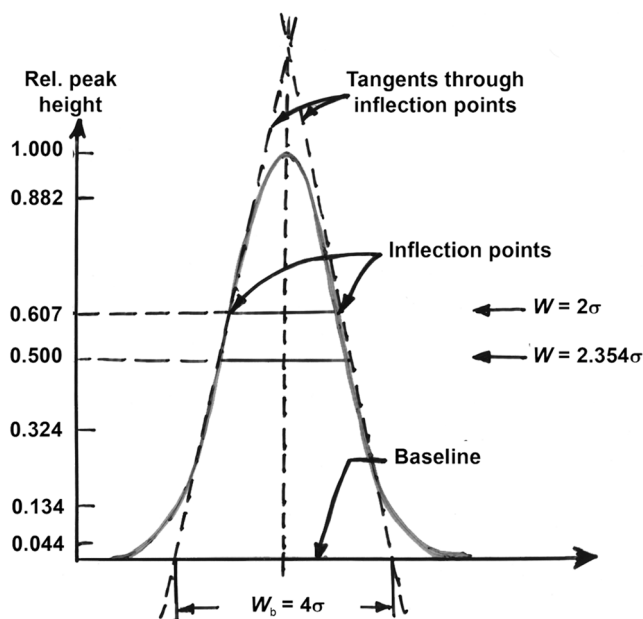


**Figure 1.2** Schematic representation of a peak with a perfect (ideal) Gaussian normal distribution. Note that the base width  $W_b$  is defined as the distance between the points

where the front and rear peak tangents cross the baseline,  $W_b$ , which corresponds to four standard deviations ( $\sigma$ ).

chromatogram and the quantitative information from the areas, or height, of the peaks (see Figure 1.1). In the ideal case, the analytical peaks are Gaussian (see Figure 1.2); however, in reality, the peaks are often slightly distorted with a small tail. The adsorption isotherms relate the mobile-phase concentration with the stationary-phase concentration (see Figure 1.3a). This relation is linear in analytical chromatography because it is performed at low concentrations corresponding to the initial, practically linear, section of the adsorption isotherm. Because of this, analytical chromatography is sometimes also called linear chromatography. In preparative separations, we instead want to purify as much as possible and the sample concentrations are normally very high, corresponding to regions where the adsorption isotherms exhibit strong curvature. In that region, a further increase of the mobile-phase concentration of the component does not lead to a proportional increase of the stationary-phase concentration. These conditions, which prevail under most preparative separations, are called nonlinear chromatography and we have severe peak deformations. If the adsorption isotherm of the component is convex upward, the resulting elution profile will have a sharp front and a diffused rear (see Figure 1.3b). But if the adsorption isotherm has the opposite shape, that is, concave upward (see Figure 1.4a), the resulting elution profile will have a diffused front and a sharp rear (see Figure 1.4b). These peak shapes are not uncommon in chiral preparative chromatography, especially

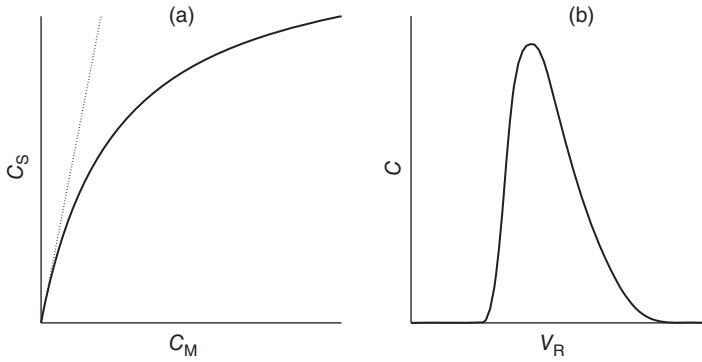


**Figure 1.3** In (a) a schematic representation of a convex upwards ("Langmurian") adsorption isotherm with the initial linear part indicated by the dotted tangent,  $C_M$  and  $C_S$  are the concentration in the mobile and

stationary phase, respectively. In (b) the shape of the resulting overloaded elution profile with sharp front and diffusive rear,  $V_R$  is the eluted volume, and  $C$  is the concentration in the eluted mobile phase at the column outlet.

when there exist an adsorbing additive in the mobile phase [4,5]. Recent research has revealed that adsorption is surprisingly complex and that advanced models often apply [6–9]. Analytical (linear) chromatography can be described by relatively simple models: injection of an  $n$  component mixture will give  $n$  Gaussian-shaped peaks, which are more or less separated in the chromatogram. Here, we focus on analytical (linear) models assuming Gaussian peaks (see Figure 1.2). The most common deviation from this in analytical chromatography is peak tailing. Figure 1.5 shows peak tailing in a schematic way and how it is measured.

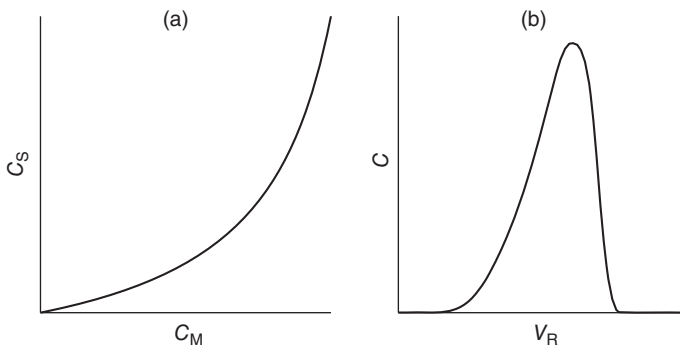


**Figure 1.4** In (a) a schematic representation of a concave upward ("anti-Langmurian") adsorption isotherm,  $C_M$  and  $C_S$  are the concentration in the mobile and stationary phase, respectively. In (b) the shape of the

resulting overloaded elution profile with diffused front and sharp rear,  $V_R$  is the eluted volume, and  $C$  is the concentration in the eluted mobile phase at the column outlet.

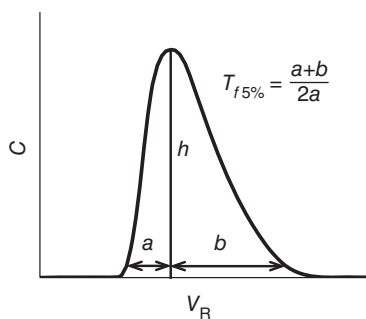


**Figure 1.5** Illustration of how the tailing factor at 5%,  $T_{f5\%}$ , is calculated from a chromatogram where  $V_R$  is the eluted volume and  $C$  is the concentration in the eluted

mobile phase at the column outlet. A line parallel to the baseline at 5% of the peak height is drawn and the distances  $a$  (front part) and  $b$  (rear part) are determined.

The pharmaceutical industry prefers to use the term tailing factor ( $T_{fx\%}$ ), which is defined in Figure 1.5, whereas in the academic community, the asymmetry factor,  $A_{sfx\%}$  ( $b/a$ ) is commonly used. In both cases,  $x$  stands for at which peak height, relative to the baseline, the asymmetry is calculated. If  $A_{sf} \sim 1$ , we have a close to “Gaussian peak,” whereas  $A_{sf} > 1$  indicates peak tailing and  $A_{sf} < 1$  indicates peak leading, alternatively called “peak fronting.”

In this context, it must be mentioned that nonlinear conditions resulting in peak tailing (see Figure 1.3b and Figure 1.5) are very common, not only in preparative chromatography but unfortunately also in analytical chromatography, since the solid phase may contain two or more different adsorption sites. If one has a few numbers of the so called “strong sites,” the curved, nonlinear, section of the adsorption isotherm is reached very early for these sites (see Figures 1.3 and 1.4) and peak tailing will occur. This is especially the case in analytical chiral chromatography [10,11] and when separating basic amines at low-to-moderate pH; here, the amines are charged leading to strong polar interactions besides the hydrophobic interactions [12,13]. Since the traditional reversed phase (= nonpolar stationary phase combined with polar mobile phase, opposite to Tswett’s original straight-phase mode) columns could not stand  $\text{pH} > 7$ , where the basic amines become more uncharged, material research was during the 1990s focused on eliminating the influence of these sites. Manufacturers investigated different ways to eliminate the strong sites during the production process, whereas academic researchers worked more on operating the existing columns in a different way, for example, to reduce the impact of the polar sample interactions by adding different competitive transparent amines in the mobile phase [14,15]. Today, hybrid materials have been introduced solving the problem in a more consistent way by allowing highly efficient silica-based stationary phases to be combined with strongly basic mobile phases [10,11,16,17]; see more below.

## 1.1.1

**Basic Retention Models and Kinetics**

A sample mixture applied on the top of a chromatographic column will be transported through the column by the mobile phase and in a properly designed column, the solutes will be eluted at the column outlet as separate zones. Now, we will look at this process in more detail and develop expressions that describe how quickly the sample zone migrates and how this can be related to the solute distribution between the mobile phase and the stationary phase.

The solutes travel can be described by the well-established relation: speed = road/time. Even if the solute zone migrates at a constant rate through the column bed, at the molecular level, the individual molecules do a “random walk.” More specifically, a single molecule transported by the mobile phase is adsorbed for a certain time and in the next moment desorbed, adsorbed again, and so on in thousands of steps during its travel along the column. We can say that the molecules behave like a bunch of rabbits on the way home through a salad field. They stop, on an individual basis, for a moment here and there to eat. On average, the individual molecule will be in the mobile phase during the time  $t_m$  and in the stationary phase during the time  $t_s$ . Its total residence time in the column becomes  $t_m + t_s$ . A molecule is adsorbed for an average time of  $t_s$ , while it is desorbed for an average time of  $t_m$ , and it then migrates with the velocity of the mobile phase,  $u_x$ . This means that the molecule will spend a fraction  $t_m/(t_m + t_s)$  of its time moving with this speed. The velocity of the molecule,  $u_s$ , is then

$$u_s = u_x \cdot \frac{t_m}{t_m + t_s} \quad (1.1)$$

Shortly after the sample starts to travel, the distribution equilibrium of the solute between the stationary phase and the mobile phase is established. If we consider a limited part of the column and assume that it represents the solute molecules' average behavior, we will have a certain amount of solute in the stationary phase,  $Q_s$ , and a certain amount in the mobile phase,  $Q_m$ . The total amount in the zone will be  $(Q_m + Q_s)$  and the percentage of the solute that is in the mobile phase is  $Q_m/(Q_m + Q_s)$ . There must be a direct correlation between the amount in the zones in the mobile phase and the corresponding time fraction for the solute in the mobile phase. The larger fraction of time the solute spends in the mobile phase, a correspondingly larger quantity is present in the mobile phase. This gives

$$u_s = u_x \cdot \frac{Q_m}{Q_m + Q_s} = u_x \cdot \frac{1}{1 + Q_s/Q_m} = u_x \cdot \frac{1}{1 + k} \quad (1.2)$$

Here,  $k$  is the *retention factor*. The definition of  $k$ , assuming the conditions are the same throughout the chromatographic bed, is given by the following simple relation:

$$k = \frac{\text{total amount of solute in the stationary phase}}{\text{total amount of solute in the mobile phase}} = \frac{C_s \cdot V_s}{C_m \cdot V_m}. \quad (1.3)$$

Thus, since the amount (moles) is equal to the concentration ( $C$ ) multiplied by volume ( $V$ ), the retention factor is simply defined as a ratio between the solute amounts in the stationary phase and those in the mobile phase. Equation 1.3 is the IUPAC definition of  $k$  [18], whereas Equation 1.4 provides an easy way to calculate  $k$  from a chromatogram:

$$k = \frac{t_R - t_0}{t_0}, \quad (1.4)$$

where  $t_R$  is the component solute retention time and  $t_0$  is the travel time for the mobile phase or the retention time of an unretained component (Figure 1.1).

### 1.1.2

#### Band Broadening and the Plate Height Concept

To perform chromatographic separation of a binary sample mixture, the two substances must have different retention times, which in turn means that they must have different distribution ratios. However, this is not the only necessary condition. Looking at a chromatogram, it is obvious that the peak widths will also affect the ability to separate one component from the other. The initially introduced solute zone must have a very narrow width, but the spreading phenomenon in the column will increase the final zone width significantly. This means that the sample molecules come out in a zone that contains a larger volume than the sample injection and this dilution increases with increasing retention factor. There are some models available that describe the effects that lead to band broadening. The easiest to understand is probably the so-called random walk model [3], which looks at band broadening as a result of a random process that exposes every molecule of movements forward or backward relative to the zone center. With a sufficiently large number of steps and molecules, the result is a normal distribution of the molecules.

The variance can be estimated from the chromatogram according to the rules for a Gaussian distribution, which states that the standard deviation in time units is  $\sigma_t = W_t/4$ , where  $W_t$  is the base width of the peak defined by the tangents to the inflection points (see Figure 1.2). The relationship (expressed in time units) between the width of the peak,  $W_t$  and the variance  $\sigma_t^2$  is then

$$\sigma_t^2 = \left( \frac{W_t}{4} \right)^2. \quad (1.5)$$

Since the variance of the peak increases with the number of steps, which is proportional to the distance migrated,  $L$ , a quantity  $\sigma^2/L$  ( $\sigma$  expressed in length units) is used as a general measure of band broadening (i.e., the efficiency of the column). It is usually called plate height (or “height equivalent to a theoretical plate”),  $H$ :

$$H = \frac{\sigma^2}{L}. \quad (1.6)$$

Do not get confused by the expression “plate height” that is used for historical reasons, consider it simply as a quantity that is proportional to the variance.

If we have several different types of random processes that occur independently and with different step lengths and number of steps, the end result is a composite profile that also is Gaussian, with a total variance that is the sum of the variances of each individual process (random walk). So, in accordance with the law on summation of variances

$$\sigma^2 = \sigma_1^2 + \sigma_2^2 + \sigma_3^2 + \sigma_4^2 + \dots \quad (1.7)$$

The corresponding expression for the summation of the individual contributions to the plate height will then be

$$H = \frac{\sigma^2}{L} = \frac{\sigma_1^2}{L} + \frac{\sigma_2^2}{L} + \frac{\sigma_3^2}{L} + \dots = H_1 + H_2 + H_3 + \dots \quad (1.8)$$

The variance also increases with the travel time of the zones, so normalization has to be done if you measure variance in time units based on the simple expression  $\text{time} = \text{path}/\text{speed}$ . The relationship between the base width of the peak in time units,  $W_t$ , and  $H$  is then obtained from

$$\sigma^2 = (\sigma_t \cdot u_s)^2. \quad (1.9)$$

So, how do we go from the definition of the plate height to an expression that can be used to calculate the plate height directly from a chromatogram? Let us first take a look again at the schematic representation of a Gaussian peak in Figure 1.2. This schematic figure shows that if you calculate the width of the peak at the base, as defined by the tangents of the slope of the rear and the front of the peak crossing the baseline, the peak width contains four standard deviations, that is,  $4\sigma$ . By combining the definition of  $H$  in Equation 1.6 with Equation 1.9, with the assumption of ideal Gaussian shape, where  $W_t = 4\sigma$ , we obtain an equation to calculate  $H$  directly from the chromatogram:

$$H = \frac{W_t^2 \cdot L}{16 \cdot t_R^2}. \quad (1.10)$$



$H$  can thus be calculated from the base width, retention time, and column length.  $H$  will be in length unit and can apparently be attributed to the width of the peak relative to its retention time. If the ratio is constant, then  $H$  is constant, assuming the same column length,  $L$ .

A measure of the *efficiency of the column as a whole* is given by the number of plates,  $N$ :

$$N = \frac{L}{H} = \frac{16 \cdot t_R^2}{W_t^2} \quad (1.11)$$

$N$  gives the total number of theoretical plates for a certain column length. Since  $N=L/H$ , the number  $N$  says something about the potential performance of a certain column where  $H$  is a more general property.

For columns with the same length, the higher the number of plates, the lower the peak width expressed as a fraction of the retention time. For a column with 1 600 plates, the peak width is 10% of the retention time, while 6 400 plates are obtained for a peak that has a width that is 5% of the retention time.

### 1.1.3

#### Sources of Zone Broadening

There are mainly three different physicochemical phenomena that cause zone broadening, graphically illustrated in Figure 1.6. The three different physicochemical phenomena are as follows:

- 1) Eddy diffusion (multiple paths)
- 2) General molecular diffusion
- 3) Slow equilibration.

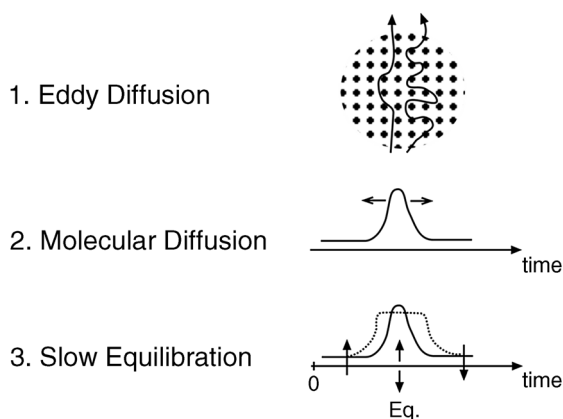


**Figure 1.6** Illustration of the three major contributions to band broadening in chromatography: (a) eddy diffusion, (b) molecular diffusion, and (c) slow equilibration.

### 1.1.3.1 Eddy Diffusion

This type of zone broadening is due to the uneven path lengths and velocities in the packed column (see Figure 1.6). It is due to the fact that as the mobile phase is pumped through the column, the flow will pass between the particles using different paths with different local flow rates and molecules trapped in these different paths will travel at different speeds. In the random walk of a solute molecule, the length of the step,  $l$ , is assumed to be equivalent to the diameter of a stationary phase (support) particle,  $d_p$ . The number of steps,  $n$ , is equal to  $L/d_p$ , that is, the length of the migration zone divided by the length of each step. This gives

$$\sigma_E^2 = l^2 \cdot n = 2 \cdot \lambda \cdot d_p \cdot L. \quad (1.12)$$

The factor,  $\lambda$ , depends on the structure of the packing; a more homogeneous packing has a lower number.

The derivations applied for the other mechanisms of band broadening by the random walk model is not given here. The readers can consult [3] for details.

### 1.1.3.2 Molecular Diffusion

This type of diffusion occurs in all directions, but since the separation occurs in the flow (axial) direction, the longitudinal diffusion has generally the largest impact on band broadening (see Figure 1.6). Diffusion also happens in the pores of the stationary phase, but the diffusion in the bulk of the mobile phase dominates. The variance,  $\sigma_D^2$ , is

$$\sigma_D^2 = \frac{2 \cdot D_m \cdot L}{u_x}, \quad (1.13)$$

where  $D_m$  is the diffusion coefficient of the solute in the mobile phase. We see that the variance for molecular diffusion contributes mainly to the band broadening at low flow rates, and increases with increasing diffusion coefficient (larger for smaller molecules) in the mobile phase.

### 1.1.3.3 Slow Equilibration

During the sample transport through the chromatographic bed, local distribution equilibrium is established in which molecules are constantly adsorbed and desorbed by the stationary phase. This process is almost always fast enough to establish equilibrium, except in those areas of the sample zone where the sample concentration changes more drastically, that is, at the front and at the back of the sample zone. At the front of the zone, higher concentration of sample molecules is pushed in all the time and the local equilibrium at the front does not have time to be established (Figure 1.6). Therefore,  $C_m$  becomes high and  $C_s$  low, and thus the ratio  $C_s/C_m$  (in Equation 1.3) is lower compared to an established equilibrium. This means that the retention factor  $k$  locally becomes small (see Equation 1.3) and thus the speed of the front zone becomes high. In the back of the zone, the opposite happens:  $C_s$  becomes high and thus  $k$  in this zone is high. In this way, the zone will broaden in both directions. Equation 1.14 gives

an expression for the variance due to this source of band broadening assuming a partitioning of solutes into the pores with an average depth of  $d_f$  and a packing factor,  $q_s$ , which is smaller with increasing homogeneity of the packing, and  $k$  is the retention factor:

$$\sigma_c^2 = \frac{k \cdot q_s \cdot d_f^2 \cdot u_x \cdot L}{D_s(1+k)} \quad (1.14)$$

An important conclusion from the variance due to slow equilibration is that it increases with the mobile-phase velocity ( $u_x$ ) and decreases with the higher diffusion/adsorption constant in the stationary phase ( $D_s$ ).

#### 1.1.4

#### Dependence of Zone Broadening on Flow Rate

In the total zone broadening, the variances of the individual sources for band broadening, as described above, are added. The relation between the total zone broadening and the linear flow rate is important and has been described with different degrees of complexity in the literature. The simple expression for packed gas chromatography (GC) by van Deemter [19] is still used as a didactic introduction to the area and also for liquid chromatography (LC). The relationship is illustrated in Figure 1.7 (solid line); it shows that there exists an optimal

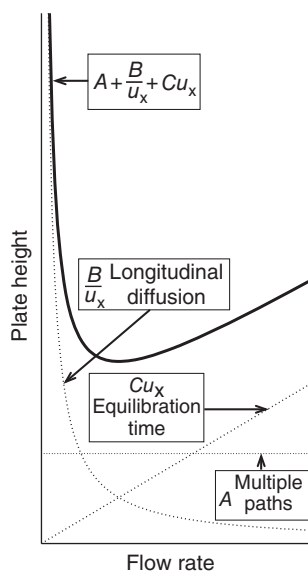


**Figure 1.7** Illustration of the three different sources for band broadening with increasing flow rate (dotted lines). The solid line shows the sum of the three individual contributions in accordance with Equation 1.15.

flow rate which gives a minimum plate height,  $H$ . This flow rate should be used to obtain the maximal number of theoretical plates ( $N$ ) for the column.

Let us take a look at Equation 1.15 and the expression derived by van Deemter for the relationship between  $H$  and the linear flow rate  $u_x$ :

$$H = A + \frac{B}{u_x} + C \cdot u_x. \quad (1.15)$$

Here,  $A$  represents eddy diffusion,  $B/u_x$  molecular diffusion, and  $Cu_x$  slow equilibria. This relationship is illustrated in Figure 1.7: the solid line at the top shows the total band broadening that is the sum of the three dashed lines below that shows the three different sources of band broadening. From Figure 1.7 and Equation 1.15, we can see that at low flow rates, the molecular diffusion is the dominating source for the band broadening, whereas at high flow rates it is the slow equilibrium that is the main reason. At the optimum flow rate, the band broadening is mainly caused by the eddy diffusion that can be decreased only by decreasing the particle sizes. Figure 1.7 is a didactic example, based on the situation in packed GC columns. In LC, the minimum is often at very low flow rates since the influence of diffusion in the mobile phase ( $B/u_x$ ) is very small as the diffusion coefficients in a liquid phase are more than 100 times lower than in a gas phase.

## 1.2 Resolution

The selectivity  $\alpha$  between two components is the ratio of the retention factors between the more retained neighboring peak ( $k_2$ ) and the less retained one ( $k_1$ ):

$$\alpha = \frac{k_2}{k_1}. \quad (1.16)$$

The selectivity is a good measure of a stationary phase ability to discriminate between two components in GC and is, for example, used by organic chemists to find the best stationary phase for separating a certain component or a class of target components. However, in LC the composition of the mobile phase also influences the selectivity, and furthermore, the selectivity does not say all about how good the separation is between two components. Here, we must find an expression that also accounts for the width of the peaks, that is, the column efficiency expressed by the number of theoretical plates. This is illustrated in Figure 1.8a–c. Figure 1.8a and c shows a chromatogram for two components with the same selectivity but different column efficiency, whereas we only have complete resolution in Figure 1.8c. Figure 1.8b has the same low column efficiency as in Figure 1.8a but much higher selectivity,  $\alpha$ , and this is another way to achieve resolution starting out from the nonresolved situation in Figure 1.8a.

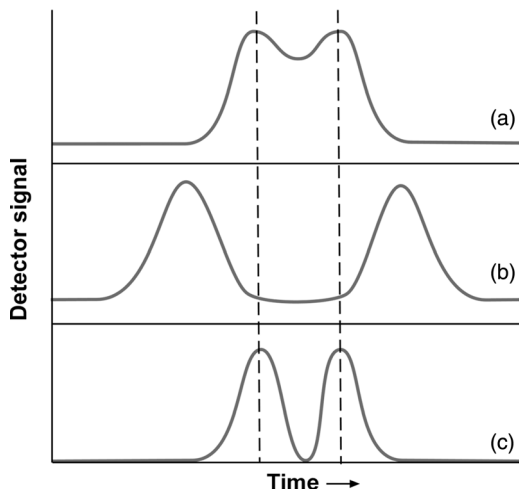


**Figure 1.8** Illustration of different ways to improve the separation of two components where we have both low efficiency and selectivity (a), in (b) the selectivity is increased, and in (c) the efficiency is increased.

Thus, the ultimate measure of a successful separation between the closely eluted peaks is the *resolution* ( $R_s$ ) accounting both for the selectivity and for the column efficiency. Here, the degree of chromatographic separation, or resolution, of two adjacent solute zones is defined as the distance between the zone centers divided by the average zone width ( $W_t$ ):

$$R_s = \frac{2(t_{R,2} - t_{R,1})}{W_{t,1} + W_{t,2}} \quad (1.17)$$

For closely adjacent bands, the average zone width is approximately equal. Since  $W_t = 4\sigma_t$ , Equation 1.17 can be written:

$$R_s = \frac{t_{R,2} - t_{R,1}}{4\sigma_t} \quad (1.18)$$

When  $R_s = 1$ , there are four  $\sigma$  units between the zone centers. This corresponds to a 2% contamination of each band by the other.  $R_s = 1.5$  corresponds to a distance of six  $\sigma$  units between the zone centers. The cross-contamination of the zones is then not more than 0.2% and the separation is almost complete, provided that the amount of solute in the two zones is approximately equal.

Now, we have a quantitative measure of the degree of resolution between the two substances and by the definition of the resolution, we understand that it depends on both the sample retention and the band broadening. Through theoretical analysis, one can show the following:

$$R_s = \frac{\sqrt{N}}{4} \cdot \left( \frac{k_2}{1+k_2} \right) \cdot \left( \frac{\alpha-1}{\alpha} \right), \quad (1.19)$$

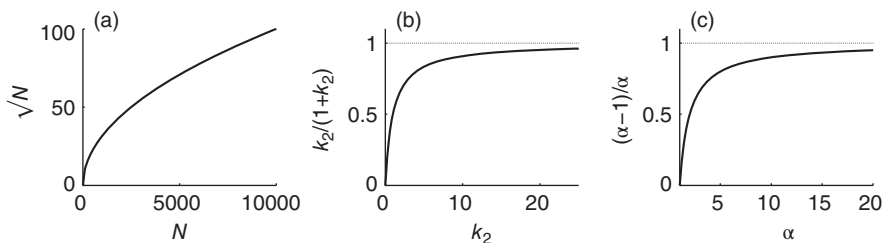


**Figure 1.9** The influence on resolution when increasing (a) the efficiency, (b) the retention factor for second component, and (c) the separation factor (see Equation 1.19).

where we know that the resolution depends on the column efficiency  $N$ , the retention factor for the more retained neighboring peak,  $k_2$ , and the selectivity,  $\alpha$ . A closer study on the effects of these different parameters on resolution will help us understand, control, and improve the resolution. As we can see, Equation 1.19 consists of three multiplied terms. Figure 1.9a–c illustrates, for each of these three terms, how a variation of the corresponding parameter affects each of these terms individually. From Figure 1.9a, we see that increasing the efficiency will continuously increase the resolution since it is proportional to the square root of  $N$ . Increasing the retention factor has a large effect when going from low values but reaches a limiting value of 1 when  $k_2$  is high; the effect on resolution is very small when  $k_2 > 10$  (see Figure 1.9b). When the separation factor is increased from 1, a similar dramatic improvement of the resolution is obtained, although this effect is greatly reduced at higher  $\alpha$ -values and reaches the limit of 1 (see Figure 1.9c). However, Equation 1.19 is valid only for low values of  $\alpha$ , since when deriving it was assumed that the peak widths of the two separated peaks were approximately equal, and this is true only when the separation factor is small ( $< 2$ ).

The simplest way to improve the resolution is to increase the retention factor, since this often can be done by a simple modification of the mobile phase. This is, however, effective only when the initial retention factor is smaller than 5. An increase of  $N$  should be the next choice; the simplest way to do this is to use a longer column. But a drawback with longer columns is decreasing sensitivity, since the dilution of the peaks will increase. The best way to increase  $N$  is, therefore, to decrease the particle diameter. The most difficult way to increase resolution is to try to increase the selectivity; this generally requires a radical change of the mobile or stationary phase that in many cases gives unpredictable results.

### 1.3

#### Modern Trends in Liquid Chromatography

Separation scientists in both academy and industry always try to continuously improve their separations, starting out from the actual knowledge, and there are

several simultaneous trends in liquid chromatography today. Many of the trends are logical consequences of the basic theory we have just covered. For example, we learned from the basic theory that the resolution ( $R_s$ ) must be  $\geq 1.5$  for a complete separation between two neighboring peaks. If the resolution is 1.5, we have 6  $\sigma$  units between the peaks' zone centers corresponding to a 0.2% coelution of the two components. From Equation 1.18, we could see that the resolution depends on the efficiency ( $N$ ), the retention factor of the second eluting component,  $k_2$ , and the selectivity,  $\alpha$ . Thus, Equation 1.18 tells us that for a pair of solutes with reasonable retention factors, we could increase the resolution by improving either the selectivity or the efficiency.

One important trend is faster analysis, with higher sample throughput, as this saves time. One way to achieve this is to develop a system with higher resolution than you need and thereafter increase the flow rate. For example, by using smaller particles (sub-2  $\mu\text{m}$  particles), the resolution can be much larger ( $R_s \gg 1.5$ ) than for larger particles and one can then increase the flow rate until  $R_s$  is the same as for the larger particles. This increased flow rate will result in a significantly higher pressure; therefore, this technique was named ultrahigh-pressure liquid chromatography (UHPLC). Another way is to use a more permeable matrix material in the column packing giving a conventional pressure, which is one of the underlying reasons for the trend in monolithic materials. Yet, another way is to use core-shell particles. Next follow further details on these materials.

### 1.3.1

#### Efficiency Trend

Already in the early days of LC [2], it was realized that in order to achieve high efficiency, the use of small particles was necessary. However, it took several decades (until the 1970s) before scientists and manufacturers learned how to make small particles  $\leq 10 \mu\text{m}$ . The new technique using small particles was given the name high-performance liquid chromatography (HPLC). A step further was to decrease the number of irregular particles in favor of spherical homogeneous particles. A challenge with the smaller particles is the need to develop instruments that can be operated under higher pressures. If we look at the parameters that determine the pressure drop over the column in Equation 1.20, we can see that the pressure is inversely related to the squared particle diameter:

$$\Delta P = \phi \frac{u_x \eta L}{d_p^2}. \quad (1.20)$$

Here,  $\Delta P$  is the pressure drop,  $d_p$  is the mean particle diameter,  $\eta$  is the viscosity and  $\phi$  the column resistance factor.  $\phi$  depends on the method for packing the column and on the porosity of the packing material. This means that going from 100  $\mu\text{m}$  particles in the 1950s to 10  $\mu\text{m}$  particles in the 1970s (a 10-fold

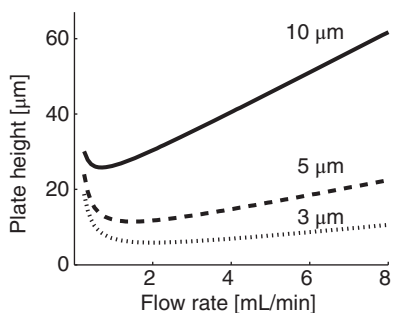


**Figure 1.10** The plate height versus the flow rate for different particle sizes: 10, 5, and 3  $\mu\text{m}$ . (Adapted from Ref. [38].)

decrease in particle size) increased the pressure drop over the column 100 times, given that all other conditions are identical.

The trend has continued with the modern sub-2  $\mu\text{m}$  porous spherical particles of today (UHPLC). The optimum  $H$  is around two-particle diameters; but as discussed above, the pressure increases inversely proportional to the square of the particle diameter (Equation 1.20). Note that increasing the mobile-phase linear velocity,  $u_x$ , also increases the pressure and the column efficiency; see Equations 1.15 and 1.20.

Figure 1.10 shows the van Deemter curves (see Equation 1.15) for the three different particle sizes: 10, 5, and 3  $\mu\text{m}$ . More specifically, Figure 1.10 illustrate that with decreasing particle sizes, the  $A$  term and  $C$  term in Equation 1.15 will decrease due to shorter irregular longitudinal path length and reduced diffusion distance. This leads to higher optimal mobile-phase linear velocity, that is, the linear velocity where  $H$  has a minimum. For example, if the particle size is decreased in an already established method, the method can be operated under larger linear velocity achieving the same efficiency (and thus maintained  $R_S$ ) using shorter columns. Reducing the particle size will not only increase the separation speed but also increase the sensitivity as the sample zone(s) get less diluted in the shorter column, provided the same injected volume is used. Because of the limited operational pressure for HPLC (400 bar), the full potential of reduced particle size cannot be utilized. As a consequence, the column length has also been decreased with decreasing particle size to operate the separation system within the pressure limit, leading to nonsubstantial increases in efficiency. Today, up to 1000 bars can be delivered by new commercial HPLC systems, called UHPLC. They first became commercially available in 2004 (Waters Acquity UPLC) [20] and shortly afterward most manufacturers offered similar equipment.

UHPLC provides faster separations with lower solvent consumptions compared to HPLC with preserved column efficiency [21,22]. Its popularity has grown steadily and UHPLC is today well-established in the pharmaceutical



industry. From an instrumental perspective, the main difference between HPLC and UHPLC is that smaller particles are used in UHPLC ( $< 2 \mu\text{m}$  particles). As a consequence, pumps able to manage pressures up to 1000 bar are required, compared to around 100–250 bar for conventional HPLC ( $\geq 3 \mu\text{m}$  particles). UHPLC is nevertheless a success story because the manufacturing companies have succeeded in producing small-particle stationary phases with very similar properties as the ones with HPLC size particles.

However, at high flow rates, there is a serious risk that the use of the reduced particle size in UHPLC leads to temperature gradients in the column that can seriously affect the chromatographic performance, that is, retention, efficiency, and resolution. More specifically, when these columns are operated at high flow rates, and thus with high inlet pressures, heat is generated in the column due to viscous friction that causes both axial and radial temperature gradients. Consequently, these columns become heterogeneous and several physico-chemical parameters, including the retention factors and the mass transfer kinetics parameters of the analytes, are no longer constant along and across the column. This has been demonstrated theoretically with advanced modeling, which combines the heat and mass balance of the column, and verified experimentally by Kaczmarski *et al.* [23,24].

In this context, it should be mentioned that a good way to decrease the pressure drop over the columns is to increase the column temperature. In accordance with the classic Equation 1.21 that follows, we can easily see that the viscosity decreases significantly with increased temperature,  $T$ :

$$\eta = A^{(Ev/kT)}, \quad (1.21)$$

where  $A$ ,  $Ev$ , and  $k$  (Boltzmann's constant) are constants. From Equation 1.20, we see that the pressure drop over the column is proportional to the viscosity. To summarize, higher temperature leads to a smaller viscosity (Equation 1.21) that in turn leads to lower pressure drop over the column (Equation 1.20). Therefore, in practice UHPLC systems are operated at somewhat elevated temperatures; often  $40^\circ\text{C}$  instead of  $25^\circ\text{C}$  used in HPLC.

### 1.3.2

#### Permeability Trend

The use of the so-called semiporous material (also called fused core particle technology, superficially porous material, or core–shells) is a strong trend today. This is another way to achieve high-efficiency separations, with higher resolution than necessary, which means one can increase the flow rate to obtain speedier analysis. From a technical perspective, the “pellicular material” introduced in 1967 [25] consisted of a solid core covered with a porous shell. The “pellicular” material did not become popular immediately, because in the 1970s the more competitive  $10 \mu\text{m}$  porous silica particles were introduced. Figure 1.11a–c illustrates the principle for semiporous packing materials. Figure 1.11a shows a modern standard HPLC particle, that is, a fully porous  $3 \mu\text{m}$  diameter particle with a

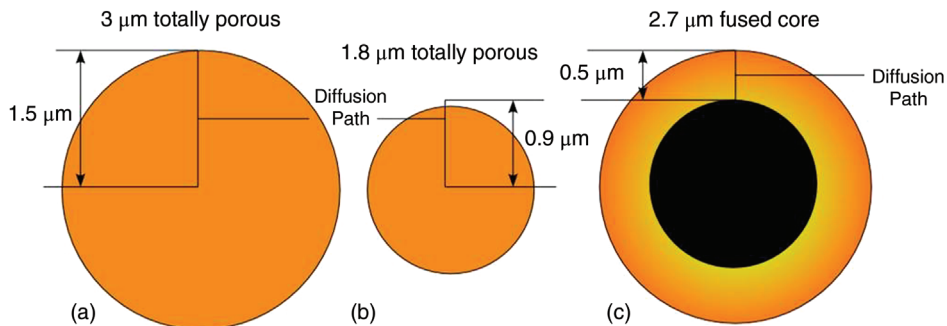


**Figure 1.11** An illustration of how fused core particles (c) as related to modern standard HPLC (a) and UHPLC (b) particles. Note that the fused core particles have shorter diffusion paths (0.5 μm) compared to HPLC (1.5 μm) and UHPLC (0.9 μm). (Adapted from an illustration provided by HALO Ltd.)

radius of 1.5 μm. Figure 1.11b shows a modern UHPLC particle, that is, a totally porous 1.8 μm diameter particle with a radius of 0.9 μm. The radius of these particles gives the maximum diffusion length that a molecule has to travel to interact fully with the particle surface. Finally, Figure 1.11c shows the so-called semiporous (or superficially porous) packing material. This particle has a porous 0.5 μm layer on top of a 1.7 μm fused core that gives a 2.7 μm particle size. This means that the use of semiporous particles results in relatively moderate pressure drops, almost comparable to standard HPLC particles since the total particle size is almost the same (2.7 μm compared to 3 μm). But at the same time, the efficiency is very high because of the short diffusion length for semiporous particles compared to UHPLC particles (0.5 μm versus 0.9 μm). The shorter diffusion length increases the mass transfer kinetics (smaller  $C$  term in Equation 1.15) and thus decreases the band broadening. Figure 1.12 shows the relation between the pressure drop over the column (in bar) and the mobile-phase velocity (in millimeter per second) for three different particle sizes 1.7 μm UHPLC packing material, 2.7 μm fused core material, and 3.6 μm standard HPLC packing material particles.

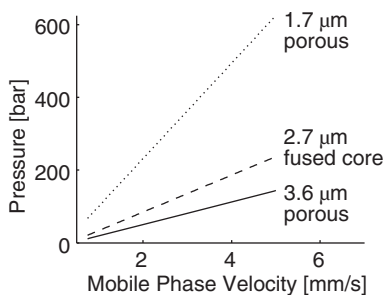


**Figure 1.12** The pressure drop across a column when different particle sizes and particle types. (Adapted from an illustration provided by HALO Ltd.)

To summarize, semiporous materials can be used with standard HPLC instruments since they have almost the same size as standard particles; this is in contrast to sub-2  $\mu\text{m}$  porous particles where the low-permeability forces the user to invest in UPLC systems. At the same time, the increased mass transfer for semiporous materials (due to shorter diffusion distances for semiporous particles, see Figure 1.11) will give very high efficiency.

Monoliths provide another solution to increase the permeability by increasing the external porosity [26,27]. Monoliths consist of single continuous porous materials, polymerized *in situ* and covalently bound to the column wall, with large through-pores that allow the flow to percolate with a convective flow through the pores and with diffusive smaller pores to increase the surface area. One disadvantage is that it is difficult to polymerize very wide and very narrow columns in a reproducible way. However, the increased permeability allows the user to employ longer columns to obtain higher column effectiveness or increased flow rates for shorter analysis times.

For monolithic columns, the  $C$  term in Equation 1.15 is much smaller than for standard HPLC packing due to shorter diffusion distances. However, the  $A$  term is larger probably because of the large-size distribution of the through-pores. Chromolith (Merk) was the first commercially available silica rod monolith column with efficiency comparable to that provided by 5  $\mu\text{m}$  particles and with a high permeability similar to a column packed with 10–15  $\mu\text{m}$  particles. Monolithic column materials are especially well suited for peptide separations.

### 1.3.3

#### Selectivity and New Material Trend

One big problem since the birth of HPLC has been the peak tailing of basic amines that adsorb on low-capacity, strongly polar (charged interactions) adsorption sites on otherwise reversed phase material. The  $\text{p}K_{\text{a}}$  of an aliphatic amine is around 9 and thus the sample components are charged at the mobile-phase pH usually used in reversed phase LC, that is, between 2 and 7. If the pH is increased above 7, the silica matrices will be destroyed. However, from a theoretical standpoint, it makes sense to separate amines at pH around 11 since the amines will be uncharged and no charged interaction with the stationary phase will occur; therefore, many attempts have been made to strengthen the silica matrix in different ways. Today, newly developed silica stationary phases, the so-called hybrid phases, are available that are stable at a pH between 1 and 12, under reversed phase LC (RPLC) conditions. The pH-stable silica was mentioned already in the 1970s and is actually a hybrid material that consists of a combination of silica and organic polymers [28]. The hybrid materials available on the market today use methyl or ethyl groups distributed throughout the particle (Xterra and XBridge from Waters) [29] or surface-grafted ethyl bridged (Gemini from Phenomenex). The stability is increased because the Si–C bond can withstand hydrolysis much better than the Si–O bond. The Xbridge particles are prepared from tetraethoxysilane and

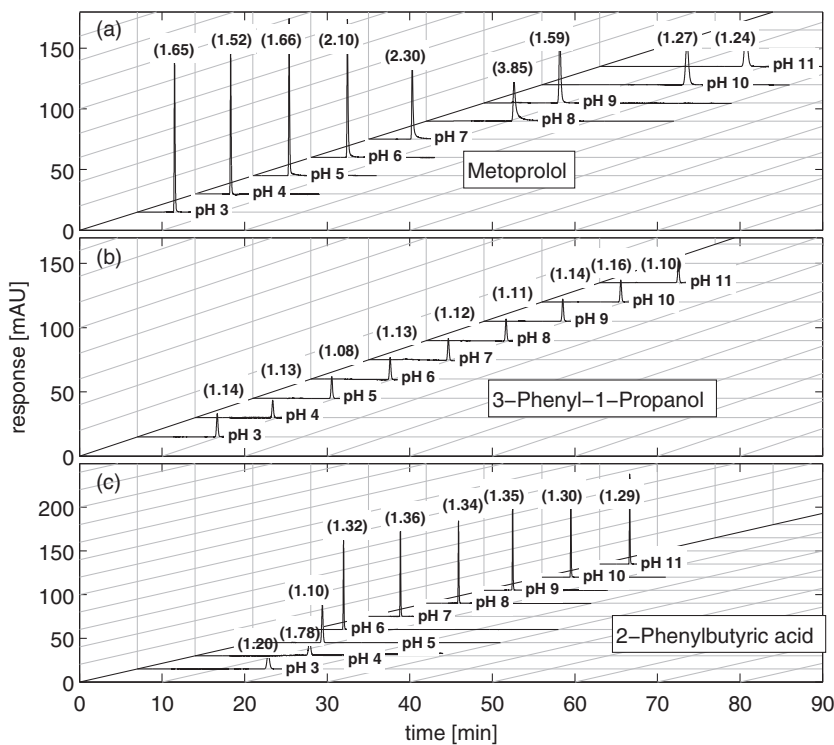


**Figure 1.13** Analytical chromatograms for (a) metoprolol, (b) 3-phenyl-1-propanol, and (c) 2-phenylbutyric acid for pH 3–11 using an XBridge column. The asymmetry values at 10% of the peak height are shown in parenthesis. (Reprinted from Ref. [10], with permission from Elsevier.)

bis(triethoxysilyl)ethane. The column lifetime is reduced at low pH due to acid hydrolysis of the bound alkylsilane. Bulky side groups on the alkylsilane have shown to sterically shield the bound siloxane from acid hydrolysis [30,31]. Hybrid materials and bidentate-bound stationary phases also seem to increase the stability [32]. Figure 1.13a–c shows the resulting eluted analytical peaks at a wide range of pH used in the mobile phase all the way from pH 3 to pH 11 using an early generation of pH-stable hybrid column (XBridge). Figure 1.13a shows the resulting peaks for a basic amine (metoprolol), Figure 1.13b for the neutral component 3-phenyl-1-propranolol (PP) and Figure 1.13c for the acidic component 2-phenylbutyric (PB) acid. The asymmetry factors ( $A_{s10}$  values) are shown in parenthesis. In the case of the neutral PP, it can be noted that the asymmetry is constant over the whole studied pH range (3–11). In the case of the acid PB, the asymmetry factor is approximately unity for all pH values, because at higher pH values, the retention time is very short. For the base ME, the asymmetry factor is maximal at pH 8; at lower pH, the

asymmetry is near unity and at pH 9–11, it decreases to below 2. At pH > 9, it is remarkable that we have a low degree of tailing of ME, in spite of the adsorption, and thus the retention of the uncharged component, increases tremendously (see Figure 1.13c).

The silica hybrid material has improved the chemical stability, but only for the short-term use. For the long-term use under chemically aggressive conditions and elevated temperature, only polymeric and metal oxide materials work. High-temperature separations are sometimes called green chromatography because less organic modifier or even pure water can be used as eluent. The reason for this is that the solvent strength in the eluent increases with increasing temperature, for example, a 4–5 °C increase of temperature approximately equals a reduction of 1% methanol or acetonitrile [33,34]. Also, the mass transfer and molecular diffusion increase with temperature, resulting in a lower *C* term but a higher *B* term in Equation 1.15 [35].

Another trend is the use of polar stationary phases combined with aqueous mobile phases, similar to those used in reversed phase mode, called hydrophilic interaction liquid chromatography (HILIC) [36]. The technique is especially useful for polar – neutral and ionic – components that are difficult to retain by reversed phase system. In HILIC, the retention increases with increasing content of organic solvent in the mobile phase. HILIC, therefore, has a special interest [37] due to its nearly orthogonal selectivity compared to RPLC; for example, at 30/70 water/acetonitrile using a ZIC<sup>®</sup>-HILIC column, uracil is retained more than naphthalene [36]. HILIC is also an alternative for separating organic bases, sugar, and other polar components that have low solubility in the nonpolar eluents used in normal-phase liquid chromatography (NPLC). As eluent, 5–40% aqueous buffer, mixed with polar organic solvents, primarily acetonitrile, are used. Examples of polar stationary phases are pure silica, diols, and amides, mixed modes with ion-exchangers, zwitterions, or sugars [36]. The retention mechanism is not completely understood but is believed to be a complex blend of liquid–liquid partitioning between the bulk eluent and an adsorbed aqueous layer on the stationary phase involving hydrogen bonding, electrostatic interactions, and weaker interactions (see Figure 1.14). The relative importance of the different interactions certainly depends on the chemical characters of both the solutes and the stationary phase.

## 1.4

### Conclusions

The main objective of this chapter is to provide a comprehensive description of the basic theory of liquid chromatography. This is necessary in order to understand the following chapters in the volume, where different chromatographic techniques, modes, and methods will be presented and discussed. An adequate theoretical knowledge of separation science is further important in order to understand the background to many of today's trends in chromatography that

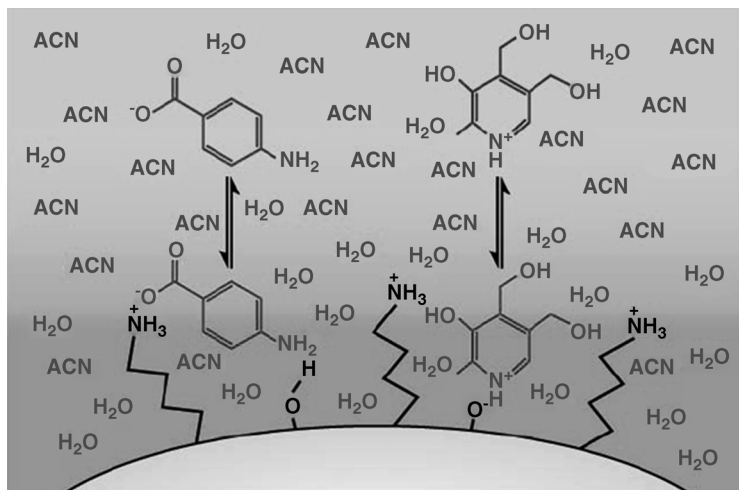


**Figure 1.14** Schematic illustration of the tentative retention mechanism in HILIC. (Adapted from an illustration provided by Phenomenex.)

are described briefly here, such as UHPLC (using  $< 2\ \mu\text{m}$  porous particles) and utilization of core-shell particles or monolithic materials in the applications of separation science. Another trend that is also presented briefly here is the development of modern pH-stable silica-based  $\text{C}_{18}$  hybrid packing materials and hydrophilic interaction chromatography.

## References

- 1 Gluckauf, E. (1946) Contributions to the theory of chromatography. *Proc. Roy. Soc. London A.*, **186** (1004), 35–57.
- 2 Martin, A.J. and Synge, R.L. (1941) A new form of chromatogram employing two liquid phases: a theory of chromatography. 2. Application to the micro-determination of the higher monoamino-acids in proteins. *Biochem. J.*, **35** (12), 1358–1368.
- 3 Giddings, J.C. (1965) *Dynamics of Chromatography: Principles and Theory*, Marcel Dekker, New York.
- 4 Arnell, R., Forsén, P., and Fornstedt, T. (2007) Tuneable peak deformations in chiral liquid chromatography. *Anal. Chem.*, **79** (15), 5838–5847.
- 5 Forsén, P., Arnell, R., and Fornstedt, T. (2009) A quest for the optimal additive in chiral preparative chromatography. *J. Chromatogr. A.*, **1216** (23), 4719–4727.
- 6 Guiochon, G., Shirazi, D.G., Felinger, A., and Katti, A.M. (2006) *Fundamentals of Preparative and Nonlinear Chromatography*, Academic Press, Boston, MA.
- 7 Felinger, A., Cavazzini, A., and Dondi, F. (2004) Equivalence of the microscopic and macroscopic models of chromatography: stochastic-dispersive versus lumped kinetic model. *J. Chromatogr. A.*, **1043** (2), 149–157.
- 8 Fornstedt, T. (2010) Characterization of adsorption processes in analytical liquid-solid chromatography. *J. Chromatogr. A.*, **1217** (6), 792–812.
- 9 Samuelsson, J., Arnell, R., and Fornstedt, T. (2009) Potential of adsorption isotherm measurements for closer elucidating of binding in chiral liquid chromatographic phase systems. *J. Separ. Sci.*, **32** (10), 1491–1506.

- 10 Samuelsson, J., Franz, A., Stanley, B.J., and Fornstedt, T. (2007) Thermodynamic characterization of separations on alkaline-stable silica-based C<sub>18</sub> columns: why basic solutes may have better capacity and peak performance at higher pH. *J. Chromatogr. A.*, **1163** (1–2), 177–189.
- 11 Undin, T., Samuelsson, J., Törnecrona, A., and Fornstedt, T. (2013) Evaluation of a combined linear–nonlinear approach for column characterization using modern alkaline-stable columns as model. *J. Separ. Sci.*, **36** (11), 1753–1761.
- 12 McCalley, D.V. (2000) Effect of temperature and flow-rate on analysis of basic compounds in high-performance liquid chromatography using a reversed-phase column. *J. Chromatogr. A.*, **902** (2), 311–321.
- 13 Ståhlberg, J. (1999) Retention models for ions in chromatography. *J. Chromatogr. A.*, **855** (1), 3–55.
- 14 Sokolowski, A. and Wahlund, K.-G. (1980) Peak tailing and retention behaviour of tricyclic antidepressant amines and related hydrophobic ammonium compounds in reversed-phase ion-pair liquid chromatography on alkyl-bonded phases. *J. Chromatogr. A.*, **189** (3), 299–316.
- 15 Tilly Melin, A., Liungcrantz, M., and Schill, G. (1979) Reversed-phase ion-pair chromatography with an adsorbing stationary phase and a hydrophobic quaternary ammonium ion in the mobile phase. *J. Chromatogr. A.*, **185**, 225–239.
- 16 Neue, U.D., Wheat, T.E., Mazzeo, J.R., Mazza, C.B., Cavanaugh, J.Y., Xia, F., and Diehl, D.M. (2004) Differences in preparative loadability between the charged and uncharged forms of ionizable compounds. *J. Chromatogr.*, **1030** (1–2), 123–134.
- 17 Davies, N.H., Euerby, M.R., and McCalley, D.V. (2006) Study of overload for basic compounds in reversed-phase high performance liquid chromatography as a function of mobile phase pH. *J. Chromatogr. A.*, **1119** (1–2), 11–19.
- 18 Nič, M., Jiráč, J., Košata, B., Jenkins, A., and McNaught, A. (eds) (2009) *IUPAC Compendium of Chemical Terminology: Gold Book*, IUPAC, Research Triangle Park, NC.
- 19 Van Deemter, J.J., Zuiderweg, F.J., and Klinkenberg, A. (1956) Longitudinal diffusion and resistance to mass transfer as causes of nonideality in chromatography. *Chem. Eng. Sci.*, **5** (6), 271–289.
- 20 Swartz, M.E. (2005) UPLC™: an introduction and review. *J. Liq. Chromatogr. R. T.*, **28** (7–8), 1253–1263.
- 21 Petersson, P. and Euerby, M.R. (2007) Characterisation of RPLC columns packed with porous sub-2µm particles. *J. Separ. Sci.*, **30** (13), 2012–2024.
- 22 Fanali, S., Haddad, P.R., Poole, C., Schoenmakers, P., and Lloyd, D.K. (eds) (2013) *Liquid Chromatography: Fundamentals and Instrumentation*, Elsevier, Waltham.
- 23 Kaczmarski, K., Kostka, J., Zapala, W., and Guiochon, G. (2009) Modeling of thermal processes in high pressure liquid chromatography. I. Low pressure onset of thermal heterogeneity. *J. Chromatogr. A.*, **1216** (38), 6560–6574.
- 24 Kaczmarski, K., Gritti, F., Kostka, J., and Guiochon, G. (2009) Modeling of thermal processes in high pressure liquid chromatography. II. Thermal heterogeneity at very high pressures. *J. Chromatogr. A.*, **1216** (38), 6575–6586.
- 25 Horvath, C.G., Preiss, B.A., and Lipsky, S.R. (1967) Fast liquid chromatography: investigation of operating parameters and the separation of nucleotides on pellicular ion exchangers. *Anal. Chem.*, **39** (12), 1422–1428.
- 26 Guiochon, G. (2007) Monolithic columns in high-performance liquid chromatography. *J. Chromatogr. A.*, **1168** (1–2), 101–168.
- 27 Vervoort, N., Gzil, P., Baron, G.V., and Desmet, G. (2004) Model column structure for the analysis of the flow and band-broadening characteristics of silica monoliths. *J. Chromatogr. A.*, **1030** (1–2), 177–186.
- 28 Unger, K.K., Becker, N., and Roumeliotis, P. (1976) Recent developments in the evaluation of chemically bonded silica packings for liquid chromatography. *J. Chromatogr. A.*, **125** (1), 115–127.

- 29 Wyndham, K.D., O'Gara, J.E., Walter, T.H., Gløse, K.H., Lawrence, N.L., Alden, B.A., Izzo, G.S., Hudalla, C.J., and Iraneta, P.C. (2003) Characterization and evaluation of C<sub>18</sub> HPLC stationary phases based on ethyl-bridged hybrid organic/inorganic particles. *Anal. Chem.*, **75** (24), 6781–6788.
- 30 Scholten, A.B., de Haan, J.W., Claessens, H.A., van de Ven, L.J.M., and Cramers, C.A. (1994) <sup>29</sup>-Silicon NMR evidence for the improved chromatographic siloxane bond stability of bulky alkylsilane ligands on a silica surface. *J. Chromatogr. A.*, **688** (1–2), 25–29.
- 31 Kirkland, J.J., Adams, J.B., van Straten, M.A., and Claessens, H.A. (1998) Bidentate silane stationary phases for reversed-phase high-performance liquid chromatography. *Anal. Chem.*, **70** (20), 4344–4352.
- 32 Kirkland, J.J. (2004) Development of some stationary phases for reversed-phase HPLC. *J. Chromatogr. A.*, **1060** (1–2), 9–21.
- 33 Bowermaster, J. and McNair, H.M. (1984) Temperature programmed microbore HPLC. Part I. *J. Chromatogr. Sci.*, **22** (4), 165–170.
- 34 Chen, M.H. and Horváth, C. (1997) Temperature programming and gradient elution in reversed-phase chromatography with packed capillary columns. *J. Chromatogr. A.*, **788** (1–2), 51–61.
- 35 Yang, Y. (2006) A model for temperature effect on column efficiency in high-temperature liquid chromatography. *Anal. Chim. Acta*, **558** (1–2), 7–10.
- 36 Hemström, P. and Irgum, K. (2006) Hydrophilic interaction chromatography. *J. Separ. Sci.*, **29** (12), 1784–1821.
- 37 Alpert, A.J. (1990) Hydrophilic-interaction chromatography for the separation of peptides, nucleic acids and other polar compounds. *J. Chromatogr. A.*, **499**, 177–196.
- 38 Harris, D.C. (2007) *Quantitative Chemical Analysis*, W.H. Freeman & Co., New York, NY.